*Research article*

# Transfer learning on T1-weighted images for brain age estimation

**Haitao Jiang**[1]**, Jiajia Guo**[1]**, Hongwei Du**[1,*]**, Jinzhang Xu**[2] **and Bensheng Qiu**[1]

[1] University of Science and Technology of China, Hefei, Anhui 230026, China

[2] School of Electrical Engineering and Automation, Hefei University of Technology, Hefei, Anhui 230009, China

* **Correspondence:** Email: duhw@ustc.edu.cn.

**Abstract:** Due to both the hidden nature and the irreversibility of Alzheimers disease (AD), it has become the killer of the elderly and is thus the focus of much attention in the medical field. Radiologists compare the predicted brain age with the ground truth in order to provide a preliminary analysis of AD, which helps doctors diagnose AD as early in its development as possible. In this paper, a transfer learning-based method of predicting brain age using MR images and dataset of a public brain was proposed. In order to get the best transfer results, we froze different layers and only fine-tuned the remaining layers. We used three planes of brain MR images together to predict age for the first time and experiment results showed that the proposed method performs better than the state-of-the-art method under mean absolute error metric by 0.6 years. In addition, to explore the relationship between brain MR images of different planes and predicted age accuracy, we used three different planes of brain MR images to predict age respectively for the first time and found that sagittal plane MR images outperformed two other planes in age estimation. Finally, our research identified, the effective regions that contribute to brain age estimation for cognitively normal individuals and for AD patients with deep learning. For AD patients, the effective region is mainly concentrated in the frontal lobe of the brain, verifying the relevant medical conclusions about AD.

**Keywords:** Alzheimer's disease; brain age; MR images; transfer learning; frontal lobe

## 1. Introduction

Various studies have shown that the morphological structure of the brain will change with the age of a human being. Moreover, some neurodegenerative diseases (e.g., Alzheimers, Parkinsons) are related to the degree of atrophy in the brain, accelerating the process of aging and brain atrophy [1]. When a person suffers from AD, his memory will begin to deteriorate, which may lead him to lose his way. As the disease worsens, memory difficulties become more and more serious, resulting in the person not
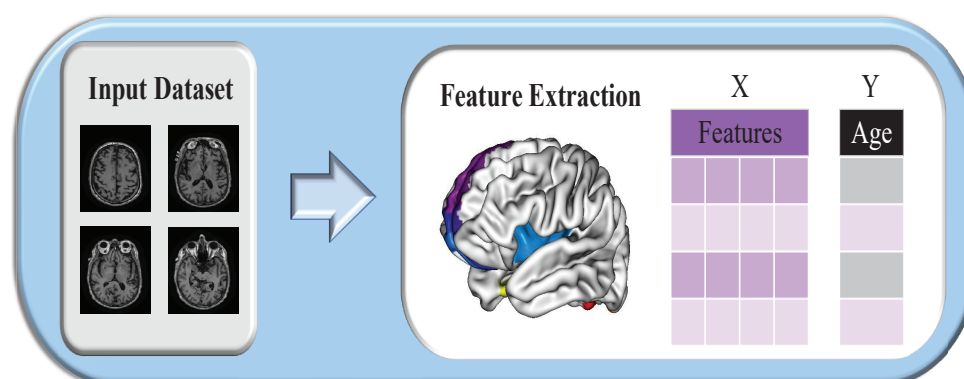
**Figure 1.** General process for brain age estimation.

being able to recognize his family members nor manage the tasks of daily life without the assistance of others. If doctors can diagnose a person with AD as early as possible and treat it effectively, it will be helpful for both the patient and his family. As we know, the brain age of a person suffering from AD is greater than his true age. If the predicted age is much older than the actual age, radiologists need to make a further diagnosis of the patient to determine if he or she has AD.

It is challenging for an experienced radiologist to predict brain age using neuroimaging data without computer technology. Therefore, doctors need to find a tool that helps them analyze medical data and get results quickly. Recently, developments in artificial intelligence (AI) technology have led it to be widely used in medical fields, such as medical image segmentation, reconstruction, and so on [2, 3, 4, 5, 6]. So far, researchers have made some achievements in brain age prediction by combining AI technology and neuroimaging data. In general, researchers utilize the features extracted from brain MR images to predict age, as shown in Figure 1.

In traditional machine learning methods, researchers need to manually select features, so how to choose the useful features is a very challenging task [7, 8]. Besides, they also do not know which features have a positive effect on the prediction of age. Therefore, traditional machine learning-based prediction methods do not work well for this task. With the rapid development of deep learning, and because of its advantages of automatically extracting features from datasets, it has been applied to brain age prediction with good prediction accuracy. Moreover, with clinical applications using neuroimaging, it usually takes hours or days to process the medical images, while decisions regarding treatment often need to be made quickly. By using deep learning, radiologists are able to quickly obtain a persons age estimation results, making it suitable for clinical applications.

Magnetic resonance imaging (MRI) is one of the most popular techniques in disease detection due to its high resolution and accurate space positioning and the absence of discomfort to patients. Various types of images are obtained from the response signal by different weighting methods. The T1-weighted MR image is one of these weighting methods. In previous studies, T1-weighted images have often been used in age estimation because they are able to reflect the brains internal structure well. However, there are few publicly available T1-weighted brain MR datasets for elderly people because they are expensive to obtain, thereby limiting the development of brain age prediction research.

As for state-of-the-art network models (e.g., VGG, AlexNet, ResNet), they are generally trained on large-scale datasets. There is less public medical data than with natural images (in order to protect patients privacy), so it is very difficult for us to train an effective network model from scratch with a

**Table 1.** Details of some datasets.

| Data sources | Paper release time | Age (Min-Max) | No. Samples |
|---|---|---|---|
| [16] | 2015 | 20-80 | 1099 |
| [21] | 2017 | 18-90 | 2001 |
| [22] | 2017 | 20-75 | 1146 |
| [23] | 2018 | 8-22 | 983 |
| Our paper | 2019 | 60-90 | 700 |

small amount of medical data. Due to the similarities between medical images and natural images, transfer learning [9, 10] is widely used in the medical field. In transfer learning, a pre-trained network model is used as a starting point to fine-tune the network for other tasks using only a limited medical dataset. Recently, some medical researchers have applied transfer learning to the diagnosis of chest pathology and pediatric pneumonia using X-rays and CT images and have classified histopathological subtypes of rhabdomyosarcoma using MR images [11, 12, 13]. These methods all perform well, which shows that transfer learning is able to achieve very good results in medical analysis.

To the best of our knowledge, brain age estimation with transfer learning on T1-weighted MR images has not yet been explored. Therefore, in this research, we proposed a more accurate method, applying a pre-trained DenseNet-201 [14] with T1-weighted brain MR images to age estimation. The key idea of our study was to explore the relationship between images of different planes and predicted ages and show the effective regions for age estimation of those affected with AD. Finally, this paper provides three contributions:

(*i*) Three different plane images were used to predict brain age respectively for the first time, and we found that the most accurate result is obtained from sagittal plane images.

(*ii*) Through deep learning, we first found that the frontal lobe area plays an active role in the age estimation of patients with AD. This area is closely related to the brain's thinking function, which verifies the related medical research about AD.

(*iii*) We verified that transfer learning can also perform well in brain age prediction under Mean Absolute Error (MAE) and Root Mean Square Error (RMSE).

The rest of this article is arranged as follows: Section 2 introduces relevant work on brain age prediction and transfer learning in the medical field. Section 3 describes the preprocessing of data and the network structure of our model. Section 4 gives the results of the age prediction. Discussion about the experimental results and conclusion are presented in Section 5 and Section 6, respectively.

## 2. Related work

Some researchers have found that T1-weighted brain images can be segmented into several parts: gray matter (GM), white matter (WM), and cerebrospinal fluid (CSF). According to [15], with an increase in age, the volume of GM decreases, the volume of WM changes slightly, and the volume of CSF increases. Based on this, [16] utilized the volume of GM, WM, and CSF areas as features to predict a persons brain age with a relevance vector machine. In [17, 18, 19], the authors manually selected some voxels and higher-order features to predict age and were able to achieve good results.

Since 2012, deep learning has achieved great success in computer vision, for it can extract features

automatically from training data [20]. Moreover, it only takes a little time to finish different regression tasks. Based on this, [21] first applied deep learning to brain age prediction and obtained good prediction accuracy. In [22, 23], the authors used deep learning for age estimation from end to end, achieving better accuracy than traditional machine learning methods. Furthermore, compared with GM and WM, the raw T1-weighted has more noise information, which interferes with age prediction [24]. Therefore, some researchers have found that prediction accuracy can be enhanced by using only the information from WM and GM rather than raw images [25, 26].

In [16, 21, 22, 23], there were young people in their datasets, with details of these datasets shown in Table 1. With young people, there are differences in brain structure at different ages since it is still developing, making it is easy to predict their brain age. Moreover, the AD is usually associated with the elderly and rarely occurs in young people. Therefore, it may not be appropriate to train a model with a dataset containing that of young people. Thus, in our dataset, only the elderly were included. Although this better matched the true situation, this dataset was more difficult for us to work with. Furthermore, the number of datasets in their papers was larger than ours, which would be more useful for predicting age but will take more time to train the model.

## 3. Materials and method

### 3.1. Dataset

The dataset[1] used in this paper is provided by the Image & Data Archive (IDA), which is a part of the Laboratory of Neuroimaging (LONI). In addition, all datasets meet the requirements of the open-sharing policies and are with restricted-sharing policies. In this dataset, all brain MR images were the T1-weighted type and were obtained by 1.5T MR modalities over the past 10 years. The subjects of all MR images are among 60 to 90 years old and the ground truth of each MR images was determined by experienced radiologists. Age estimation is a challenging task with a wide range age distribution dataset. Furthermore, the number of subjects in this dataset between the ages of 70 and 80 was the largest, accounting for about 49%, and the ratio of male to female was about 53:47. Finally, T1-weighted brain MR images of 700 subjects with the format of NiFTI were selected to brain age estimation in our experiment. For these 700 subjects, we randomly upset their order and further divided them into three parts: training(60%), validation(20%) and test(20%). Each part of the dataset is independent of each other, thus avoiding the training dataset is applied to the process of testing.

### 3.2. Preprocessing

In previous work, these authors performed some preprocessing on the raw data to accelerate network convergence and improve accuracy. Therefore, this section describes the preprocessing in our study, which consists of three parts: segmentation, building input datasets, and data augmentation. Details are as follows. Besides, the operation of segmentation and building input datasets in preprocessing are both applied in the training set and test set, which is a necessary part. We only added data augmentation to the training set to achieve better performance.
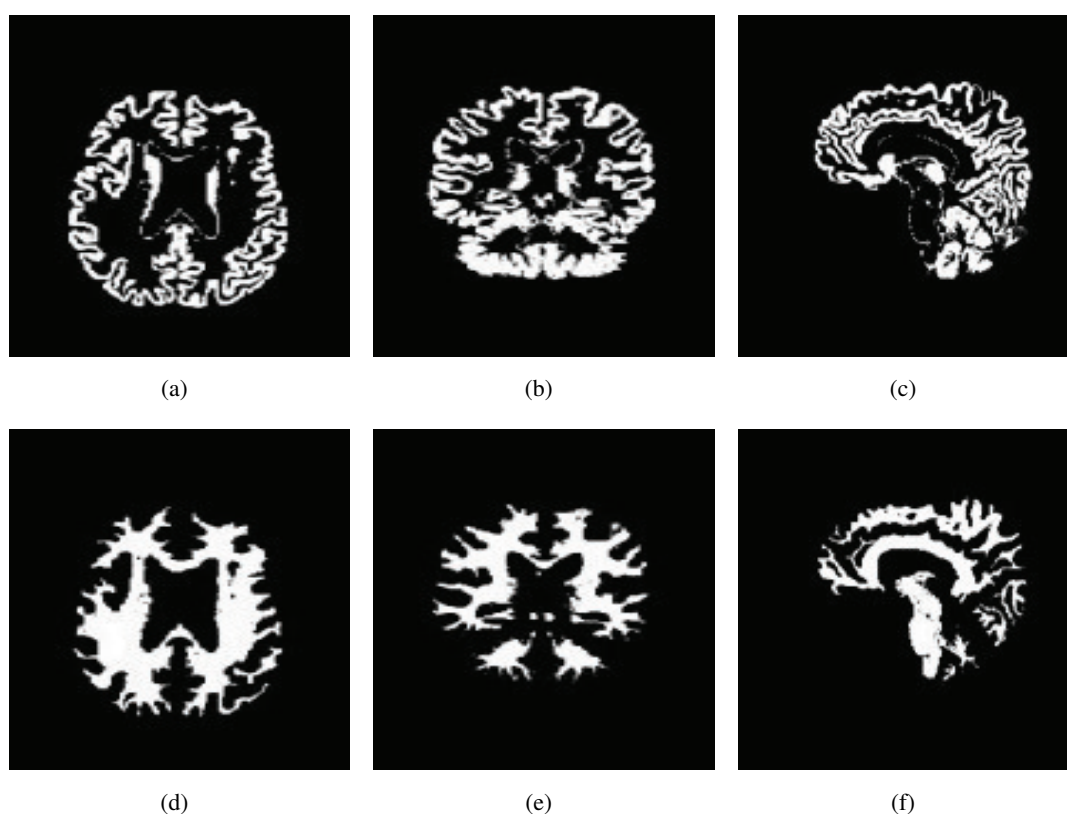
---

[1] `https://ida.loni.usc.edu/login.jsp?project=ADNI`

**Figure 2.** Images of samples in this paper: (a)-(c) represent the axial plane, coronal plane, sagittal plane of GM, respectively; (d)-(f) represent the axial plane, coronal plane, sagittal plane of WM, respectively.

### 3.2.1. Raw brain MR images segmentation

As mentioned above, raw T1-weighted brain MR images can be further segmented into WM and GM regions. Researchers have obtained more accurate estimation results with the information of WM and GM than with raw MR images. At this time, we also implemented the operation of segmentation for better accuracy, which was conducted with Statistical Parametric Mapping 2 (SPM2) and MATLAB 2014a. In comparing SPM2 with newer versions of SPM such as SPM5 and SPM8, the authors in [16] confirmed that SPM2 performed better. Thus, SPM2 was applied in this study. Finally, for each slice of segmented GM and WM images, we obtained its three different axial planes, which were recorded as slices in the order of axial plane, coronal plane, and sagittal plane, respectively, as shown in Figure 2.

### 3.2.2. Building input datasets

As mentioned in abstract, to explore the relationship between age estimation accuracy and different planes of brain MR images, we used three different planes images to predict age respectively for the first time. Besides, we also need to use the combination of three planes brain MR images to predict age. Therefore, in this section, we construct brain MR images datasets of three different planes respectively. However, some slices contained only a small amount of brain information and had little predictive
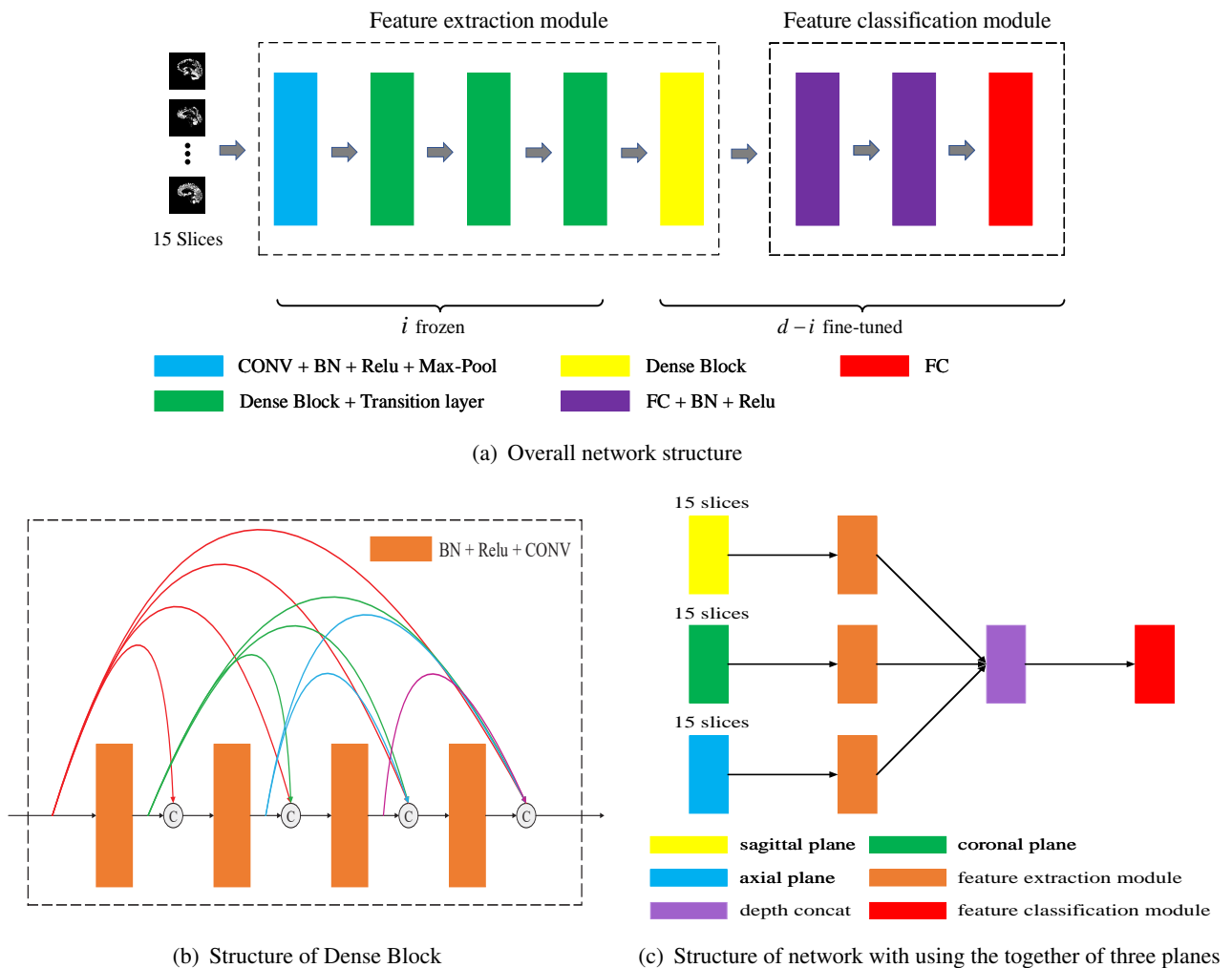
(a) Overall network structure



(b) Structure of Dense Block



(c) Structure of network with using the together of three planes

**Figure 3.** Network architecture.

value in determining brain age. For this reason, 15 slices which contained most of the brain tissue in each plane were selected as input for one subject to reduce the calculations needed in this paper. The subsequent steps were as follows:

(*i*) We obtained the total number of brain MR slices in the current plane. $T_i^a$, $T_i^c$, and $T_i^s$ represent the total number of brain MR slices in the axial plane, coronal plane, and sagittal plane of the $i$th subject, respectively;

(*ii*) We got the $\lfloor \frac{T_i^a}{2} \rfloor$th brain slice in the axial plane of $i$th subject;

(*iii*) The slice number of these: $\lfloor \frac{T_i^a}{2} \rfloor + 4 \times k$, where $k \in \{-7, -6, ..., 7\}$ were selected for input data;

(*iv*) Slice operation were performed in the three planes for each subject's GM and WM, respectively;

(*v*) Each selected slice was resized to $224 \times 224$.

Thus, we obtained an input dataset for each subject, which included three planes slices of GM and three planes slice of WM.

### 3.2.3. Data augmentation

With data augmentation, we could acquire more medical data based on the limited existing data, which not only improved the accuracy of brain age predictions but also reduced overfitting [27]. The details of the data augmentation methods implemented in this study are as follows:

(*i*) Rotating the slice between 10 degrees randomly;

(*ii*) Shifting the slice between 15 pixels randomly.

Each slice of the network input needed to be carried out using the same rotating/shifting operation in one augmentation.

### 3.3. Network architecture

DenseNet has two compelling advantages in that it encourages feature reuse and it substantially reduces the number of parameters [14], which not only lowers the requirements on the hardware device but also has the benefit of good feature extraction. Moreover, there is a similarity in edges and blobs found in both natural images and medical images, so these two types of images share some low-level features [13]. Based on this, the fine-tuning of a pre-trained DenseNet-201 was conducted to extract features for age estimation. Our architecture is illustrated in Figure 3. There were 1024, 512, and 1 neurons in three full connection layers, respectively, and the adjacent two full connection layers included a batch normalization layer [28]. In particular, the output of the last fully connected layer was a discrete number, which represented the predicted value of age. In addition, the process of max pooling was carried out with a $3 \times 3$ kernel and a stride of $2 \times 2$. There was a convolution layer with $1 \times 1$ kernel and average pooling layer with a $2 \times 2$ kernel and a stride of 2 in the transition layer. The value of $d$ represents the depth of our network, which was 6 in this study. To regularize and accelerate the convergence of the model, we added the batch normalization layer. For a mini-batch of size $n$, a sample $x_i$ can be normalized into $y_i$ after batch normalizing transform, which is presented in Table 2. Moreover, in this transform, $\epsilon$ is a constant to ensure the stability of $\overline{x}_i$ .

**Table 2.** Batch normalizing transfrom.

| |
| --- |
| **Input:** $x_i$ is the $i$-th sample of a mini-batch: $i \in \{1, 2, ..., n\}$; Parameters to be learned in the training: $\gamma$, $\beta$ |
| **Output:** $y_i = \text{BN}(x_i)$ |

| | | |
| --- | --- | --- |
| (1) | $\mu \leftarrow \frac{1}{n} \sum_{i=1}^{n} x_i$ | //mean for a mini-batch |
| (2) | $\sigma \leftarrow \frac{1}{n} \sum_{i=1}^{n} (x_i - \mu)^2$ | //variance for a mini-batch |
| (3) | $\overline{x}_i \leftarrow \frac{x_i - \mu}{\sqrt{\sigma + \epsilon}}$ | //normalize |
| (4) | $y_i \leftarrow \gamma \overline{x}_i + \beta$ | output |

### 3.4. Loss function

Loss function plays an important role in the process of training the model. MAE loss and Mean Square Error (MSE) loss, as two different types of loss functions, are widely used to solve regression problems, age prediction being one of them. Compared with MSE, MAE can better reflect the actual

situation of prediction error. MAE also performs better than MSE in related age prediction problems [29, 30]. Therefore, MAE was selected as the loss function to predict brain age in this study, which is defined as follow:

$$L_{MAE} = \frac{1}{N} \sum_{i=1}^{N} |\overline{y}_i - y_i|, \tag{3.1}$$

where $N$ is the number of the training samples, $\overline{y}_i$ is the predicted value of the $i$-th sample, and $y_i$ is the ground truth.

Regularization is an important method of reducing the risk of overfitting and improving the generalization ability of a model in deep learning. In terms of L2 regularization, it is easy to carry out and differentiable everywhere, and is thus widely used. Based on this, L2 regularization was added to the loss function in the process of training for our model.

$$L2 = \sum_{i=1}^{m} \|w_i\|_2^2, \tag{3.2}$$

where $m$ is the number of the all weights and $w_i$ is the $i$-th weight of our model.

## 4. Experiment and Results

### 4.1. Implementation environment

All experiments described in this paper were implemented in PyTorch[2]. The operating system of our computer is based on Linux and the specific version is Ubuntu 16.04. All codes were run on the Nvidia GTX 1080-Ti graphics card with 11GB GDDR5X and Intel Xeon E5-2630 v4 @ 2.20GHz.

### 4.2. Details of training

In our experiments, transfer learning was implemented by freezing the shallowest $i$ layers, and the remaining $d - i$ layers were fine-tuned. To update the parameters of the network, the Adam update rule was adopted and a rectified linear unit (ReLU) [31] was also used as a non-linearity activation function with a mini-batch of 32. We employed batch normalization in each mini-batch to normalize the output of each layer and also to speed up convergence. To avoid overfitting, a dropout rate of 0.5 was applied to the fine-tuning of our network. The learning rate refers to the magnitude of the parameter update in the original model after each epoch. The learning rate decay reduces the magnitude of parameter updates during the training process. Thus, it was also implemented in our paper. Our model was fine-tuned with a starting learning rate value of 0.0001 and learning rate decay by 0.8 every 20 epochs. Finally, a 5-fold cross-validation was used in our experiments to take full advantage of our existing medical datasets.

### 4.3. Evaluation metrics

Evaluation metrics are applied to determine whether a trained model can solve the problem well, an indispensable step in deep learning. Different deep learning tasks have different evaluation metrics.

[2]https://pytorch.org/

MAE, MSE, and RMSE are widely used as evaluation metrics in solving the problem of regression. Age estimation is one type of regression task. For MAE, it can intuitively reflect the error between the predicted value and the ground truth, which is widely used as a basic metric for age estimation [29, 30]. In [21, 32], RMSE was chosen as an additional metric to evaluate age prediction results. Because of this, MAE and RMSE were both selected as evaluation metrics to evaluate the prediction accuracy from different aspects and avoid the contingency of results in this study, which are defined as follows.

$$MAE = \frac{1}{N} \sum_{i=1}^{N} |\bar{y}_i - y_i|, \tag{4.1}$$

$$RMSE = \sqrt{\frac{1}{N} \sum_{i=1}^{N} (\bar{y}_i - y_i)^2}. \tag{4.2}$$

### 4.4. Experimental Results

In this section, we first show the various age prediction results obtained by freezing a part of the layers and fine-tuning the remaining layers. We then give the prediction error with fine-tuning all layers for different types of input datasets. Moreover, to verify that our method was more effective, it is compared to other proposed methods. Finally, some visual brain areas that have a positive effect on age estimation of cognitively normal individuals and those with AD are shown.
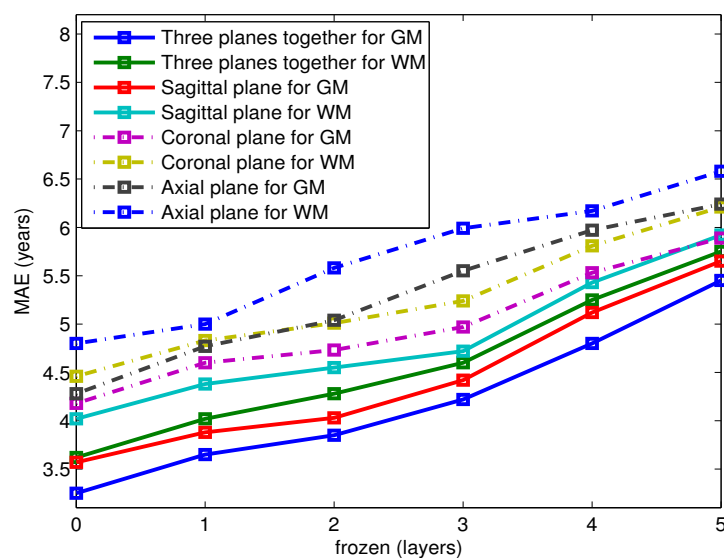


**Figure 4.** Transfer learning with freezing different layers.

### 4.4.1. Results with freezing different layers

For a pre-trained network, its parameters were learned well on a large amount of dataset. We only needed to fine-tune the pre-trained network with a specific dataset when it was applied to other tasks. However, it was not known whether the best age estimation result could be obtained by fine-tuning all the layers or a portion of the layers and the remaining layers frozen. To make the best
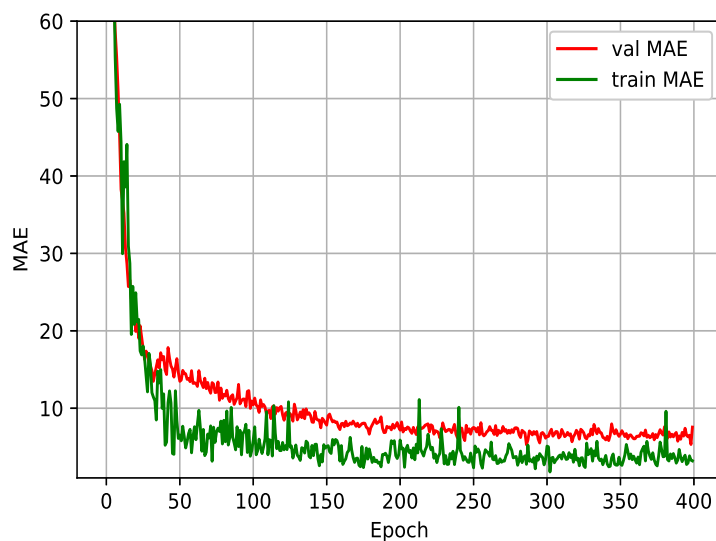
**Figure 5.** The process of fine-tuning all layers.

use of the advantages of transfer learning and obtain the best prediction result, therefore, we tried to freeze different layers and fine-tuned the remaining layers with all input datasets. Although freezing zero layers took more computational cost than all layers, we could obtain better prediction accuracy, making it worthwhile for clinical applications. Detailed fine-tuning results can be seen in Figure 4. From this figure, we can see that regardless of the type of datasets inputted, the best estimation results could always be obtained by fine-tuning all layers. In Figure 5, we provide the process of fine-tuning all layers with the input data of the sagittal plane for GM. From the process of fine-tuning, we know that our model basically converged within 300 epoch, and it did not take long to train the model.

### 4.4.2. Results of predicted age error

In Section 4.4.1, we determined that the best performance of age estimation could be obtained by fine-tuning all layers. Thus, in this section, the method of fine-tuning all layers was chosen to obtain our age prediction accuracy. We used both *MAE* and *RMSE* to evaluate the results with all types of input data. The detailed error between predicted brain age and ground truth for our network is summarized in Table 3. From the experimental results, we can know that the GM of sagittal plane performs best in age estimation under two representative evaluation metrics.

Furthermore, some comparative experiments were performed to test the effectiveness of our approach, and comparative algorithms were implemented with our dataset to ensure the fairness of the experiment. In the comparative experiments, if all types of input datasets were involved, the workload would be unnecessarily large. As shown in Table 3, the best prediction accuracy could be obtained with the together of three planes; thus, we chose the GM and WM of the combination of three planes for use in the comparison experiments. As shown in Figure 6, GM_MAE indicated that the input dataset was the GM of three planes together and the evaluation metric was MAE; the remainder could also be done in the same manner. Experimental results showed that our method performs better than other related methods under two representative metrics. Moreover, our error under MAE is about 0.6 years smaller
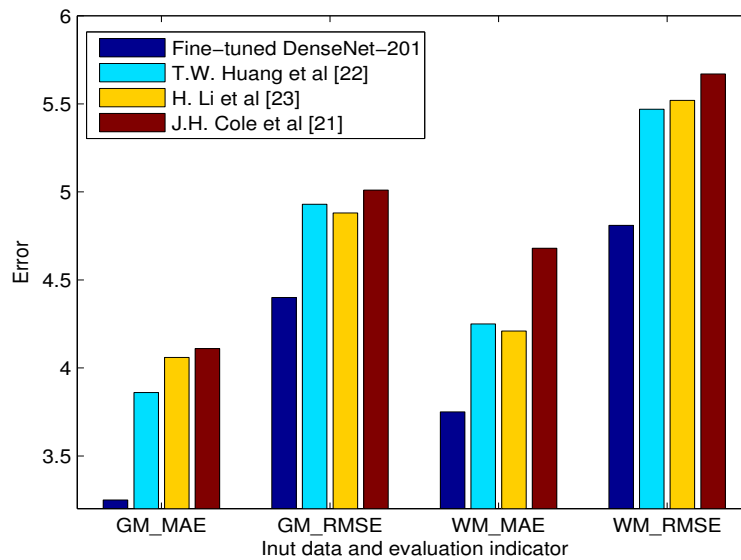
**Figure 6.** Comparative experiment of age error.

than the proposed state-of-the-art technology.

**Table 3.** Error of fine-tuned DenseNet-201.

| Input data | MAE (years) | RMSE |
|---|---|---|
| **Three planes togethter for GM** | **3.25** | **4.30** |
| Three planes togethter for WM | 3.62 | 4.81 |
| Sagittal plane for GM | 3.57 | 4.73 |
| Sagittal plane for WM | 4.18 | 5.23 |
| Coronal plane for GM | 4.02 | 4.99 |
| Coronal plane for WM | 4.46 | 5.29 |
| Axial plane for GM | 4.28 | 5.43 |
| Axial plane for WM | 4.80 | 6.19 |

### 4.4.3. Effective regions for age estimation

As previously mentioned, deep learning has achieved great success in the field of computer vision, and some researchers have applied it to age estimation with good results. One reason is that features can be extracted automatically by deep learning from training datasets. Features extracted by deep learning are more suitable for predicting age than features selected manually by researchers. Furthermore, brain age will change with the atrophy of brain. Therefore, specific to this research, the features extracted by the network during the training process are closely related to the morphological structure in some areas of the brain. In other words, there are some brain regions that have a very great contribution to age estimation. Questions for further analysis include the following:

(i) Which area of the brain plays a positive role in predicting brain age for a cognitively normal person?

(ii) What are the differences in areas actively involved in age prediction between cognitively normal person and AD patients?

With the help of visualization tools[3], we obtained the heatmap of the model output. The red regions in the heatmap are displayed in a highlighted form in Figure 7 from three different planes, visualized with the BrainBrowser Surface Viewert[4]. From the figure, we can see that for a cognitively normal person, the highlighted area is mainly concentrated in the primary motor cortex area, while for a person suffering from the AD, the area is mainly concentrated in the frontal lobe area. The experimental results show that the frontal lobe region has little contribution to age estimation for the cognitively normal person, while it has a positive impact on a person with AD.
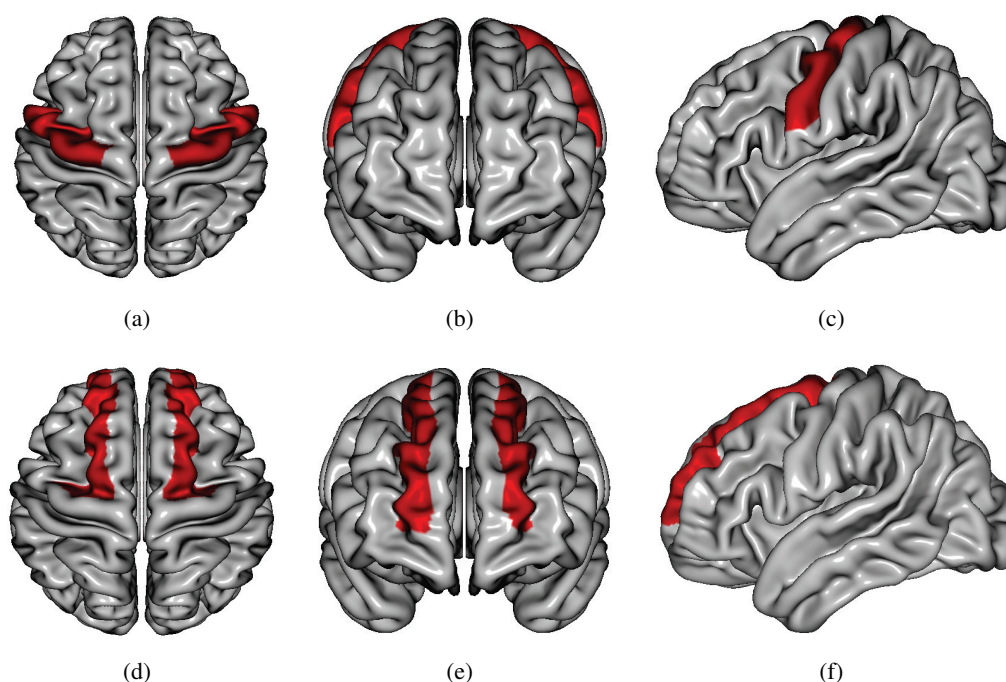


**Figure 7.** Effective regions for age estimation: (a)-(c) represent axial plane, coronal plane, sagittal plane of cognitively normal person, respectively; (d)-(f) represent axial plane, coronal plane, sagittal plane of AD patients, respectively.

## 5. Discussion

A phenomenon is found from our experimental results: we were able to get a smaller prediction error using GM as the input of our network than by using WM. This shows that in the process of age estimation, the contribution of GM is greater than that of WM. As we know, GM and WM are both important parts of the central nervous system, but they play different roles. More concretely, GM is a nervous tissue and a concentrated part of cell bodies in nerve cells and plays a positive role in the entire information-processing and decision-making process. It processes various kinds of information such as exercise, language, and emotion, and controls the body in responding accordingly. In general, if a

---

[3]`https://github.com/utkuozbulak/pytorch-cnn-visualizations`
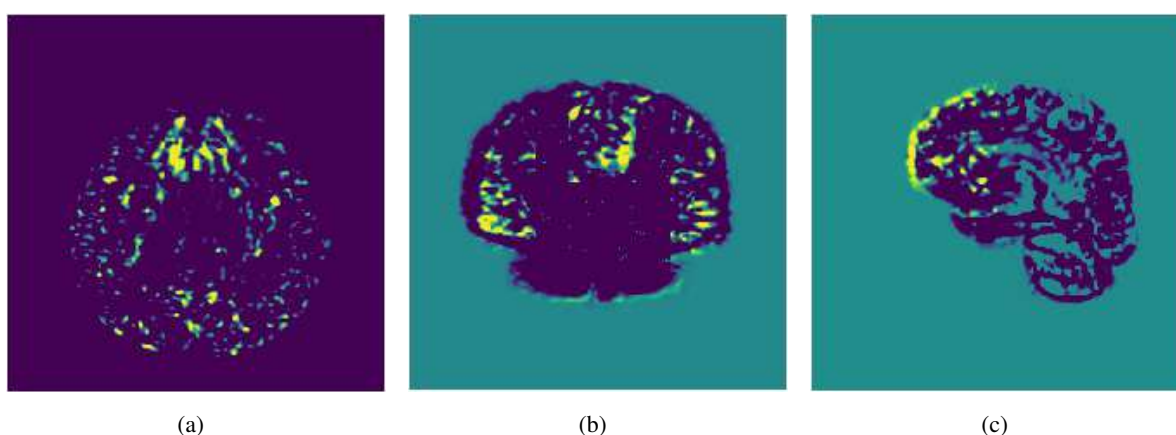[4]`https://brainbrowser.cbrain.mcgill.ca/`

**Figure 8.** Two-dimensional feature distribution: (a)-(c) represent axial plane, coronal plane and sagittal plane respectively.

persons brain becomes older, they usually tend to move more slowly, and their memory will be more attenuated, which is closely related to GM. WM is a concentrated part of nerve cells and is responsible for delivering all kinds of information to its destination. Therefore, WM is mainly involved in the transmission of information and is less involved in processing information and making decisions. In summary, GM is more closely related to the decision-making process and movement than WM, which explains why it is more suitable for predicting brain age. Besides, we found that the sagittal plane MR images outperformed two other planes in age estimation. As shown in Figure 8, this is the two-dimensional feature distribution of three different planes that is displayed by the visualization tool in Section 4.4.3. The highlighted area in this figure is the feature area. Due to the different plane of the observed brain vision is not the same, therefore, the observed feature area will also be different. From the figure, we can see that the highlighted area in the frontal lobe of the sagittal plane distributed higher than other planes. In the medical field, researchers have discovered that the frontal lobe is associated with human thinking and movement. Furthermore, thinking and movement are closely related to human physiological age, which may be the reason for using the sagittal plane images can get the best prediction accuracy. From the experimental results, we also learned that the combination of three planes MR images can get the best accuracy. As mentioned before, the observed fields of view are not the same for each plane, resulting in the difference in features extraction. Compared with using one plane, the network can observe a wider field of view at the same time with combining three planes, so that more features can be extracted. Thus, this may explain the best performance can be obtained with three planes together.

In [33], the authors state there is a relationship between AD patients and frontal lobe atrophy. They cited researchers who developed a dynamic model of atrophic disease and then found that for AD patients, atrophy of the brain begins in the temporal lobe and eventually extends to the frontal lobe. Agosta et al. [34] demonstrated that the brain of AD patients undergoes atrophy from the temporal lobe to the frontal lobe using the VBM method in their experimental results. This also shows that atrophy of the frontal lobe is a manifestation of AD disease. Furthermore, the authors of both [35] and [36] have mentioned that for AD patients, the gray matter volume in the frontal lobe region is significantly reduced. In the above studies, researchers used some traditional machining methods to verify the close

relationship between AD and the atrophy of the frontal lobe. However, no researchers have verified that there is a connection between the AD and frontal lobe atrophy through the use of deep learning.

As discussed in Section 4.4.3, we show the effective regions for age estimation with deep learning. The frontal lobe area is rarely marked as a highlighted area in the visualized images for the cognitively normal person, while for AD patients, this area is generally highlighted. This result essentially verifies two medical phenomena: (1) there is indeed a certain correlation between AD and atrophy of the frontal lobe; (2) the degree of atrophy of the brains frontal lobe is aggravated during the process of transforming from cognitively healthy to AD. For the cognitively normal person, the frontal lobe area of the brain is less atrophic, while AD patients have a large degree of atrophy. Therefore, we verified the work of predecessors regarding AD using deep learning.

## 6. Conclusion

In this study, a pre-trained network (DenseNet-201) was applied to brain age estimation. To explore the relationship between images of different planes and predicted ages, we first used three planes of brain images as the input of our network. The final experimental results show that the sagittal plane for GM gets the best result. Compared with other proposed methods, our method achieves better results under two different evaluation metrics, which verifies that transfer learning is effective in age prediction. We also show the effective regions in age estimation for cognitively normal individuals and those with AD. We find there is a difference between them in these effective regions. For a person with AD, the effective regions are closely related to the brains thinking activity, which confirms some medical analysis about AD. It will be very promising to extend AI to medical image analysis, which combines medical science with AI from the existing literature. If AI is well applied in the medical field, it can not only improve the efficiency of medical diagnosis but also play an inestimable role in promoting the development of medicine in the future.

## 7. Future work

In Section 3.2, SPM2 is used to segment the raw T1-weighted brain MR images. Then, the gray matter and white matter images obtained by segmentation are applied to brain age estimation for better prediction accuracy. Therefore, the part of segmentation is necessary for us. However, raw T1-weighted segmentation will cost a long time. Specifically, in this paper, it took about 5 minutes for a subject in the operation of segmentation. If we can shorten the split time to less than 1 minute, I think it will be a very meaningful job. Thus, we will focus on how to reduce time in segmentation with deep learning in our future work.

**Conflict of interest**

The authors declare that there is no conflict of interests regarding the publication of this article.

**References**

1. L. Pini, M. Pievani, M. Bocchetta, et al., Brain atrophy in alzheimers disease and aging, *Ageing Res. Rev.*, **30** (2016), 25–48.

2. A. Hosny, C. Parmar, J. Quackenbush, et al., Artificial intelligence in radiology, *Nat. Rev. Cancer*, (2018), 1.

3. A. Rios and R. Kavuluru, Ordinal convolutional neural networks for predicting rdoc positive valence psychiatric symptom severity scores, *J. Biomed. Inform.*, **75** (2017), S85–S93.

4. O. Ronneberger, P. Fischer and T. Brox, U-net: Convolutional networks for biomedical image segmentation, in *International Conference on Medical image computing and computer-assisted intervention*, Springer, 2015, 234–241.

5. B. Harangi, Skin lesion classification with ensembles of deep convolutional neural networks, *J. Biomed. Inform.*, **86** (2018), 25–32.

6. S. Zhang, E. Grave, E. Sklar, et al., Longitudinal analysis of discussion topics in an online breast cancer community using convolutional neural networks, *J. Biomed. Inform.*, **69** (2017), 1–9.

7. J. Xi and A. Li, Discovering recurrent copy number aberrations in complex patterns via non-negative sparse singular value decomposition, *IEEE/ACM TCBB*, **13** (2016), 656–668.

8. J. Xi, M. Wang and A. Li, Discovering mutated driver genes through a robust and sparse co-regularized matrix factorization framework with prior information from mrna expression patterns and interaction network, *BMC Bioinform.*, **19** (2018), 214.

9. J. Yosinski, J. Clune, Y. Bengio, et al., How transferable are features in deep neural networks?, in *Adv. Neural Inf. Process Syst.*, 2014, 3320–3328.

10. K. He, R. Girshick and P. Dollr, Rethinking imagenet pre-training, *arXiv preprint arXiv:1811.08883*.

11. P. Lakhani and B. Sundaram, Deep learning at chest radiography: automated classification of pulmonary tuberculosis by using convolutional neural networks, *Radiology*, **284** (2017), 574–582.

12. D. S. Kermany, M. Goldbaum, W. Cai, et al., Identifying medical diagnoses and treatable diseases by image-based deep learning, *Cell*, **172** (2018), 1122–1131.

13. I. Banerjee, A. Crawley, M. Bhethanabotla, et al., Transfer learning on fused multiparametric mr images for classifying histopathological subtypes of rhabdomyosarcoma, *Comput. Med. Imag. Grap.*, **65** (2018), 167–175.

14. G. Huang, Z. Liu, L. Van Der Maaten, et al., Densely connected convolutional networks., in *CVPR*, vol. 1, 2017, 3.

15. Y. Taki, B. Thyreau, S. Kinomura, et al., Correlations among brain gray matter volumes, age, gender, and hemisphere in healthy individuals, *PlOS ONE*, **6** (2011), e22734.

16. C. Kondo, K. Ito, K. Wu, et al., An age estimation method using brain local features for t1-weighted images, in *Engineering in Medicine and Biology Society (EMBC), 2015 37th Annual International Conference of the IEEE*, IEEE, 2015, 666–669.

17. K. Franke, G. Ziegler, S. Klöppel, et al., Estimating the age of healthy subjects from t1-weighted mri scans using kernel methods: exploring the influence of various parameters, *Neuroimage*, **50** (2010), 883–892.

18. B. Wang and T. D. Pham, Mri-based age prediction using hidden markov models, *J. Neurosci. Meth.*, **199** (2011), 140–145.

19. J. Wang, W. Li, W. Miao, et al., Age estimation using cortical surface pattern combining thickness with curvatures, *Med. Biol. Eng. Comput.*, **52** (2014), 331–341.

20. J. Xi, A. Li and M. Wang, A novel unsupervised learning model for detecting driver genes from pan-cancer data through matrix tri-factorization framework with pairwise similarities constraints, *Neurocomputing*, **296** (2018), 64–73.

21. J. H. Cole, R. P. Poudel, D. Tsagkrasoulis, et al., Predicting brain age with deep learning from raw imaging data results in a reliable and heritable biomarker, *NeuroImage*, **163** (2017), 115–124.

22. T.-W. Huang, H.-T. Chen, R. Fujimoto, et al., Age estimation from brain mri images using deep learning, in *Biomedical Imaging (ISBI 2017), 2017 IEEE 14th International Symposium on*, IEEE, 2017, 849–852.

23. H. Li, T. D. Satterthwaite and Y. Fan, Brain age prediction based on resting-state functional connectivity patterns using convolutional neural networks, in *Biomedical Imaging (ISBI 2018), 2018 IEEE 15th International Symposium on*, IEEE, 2018, 101–104.

24. A. Giorgio, L. Santelli, V. Tomassini, et al., Age-related changes in grey and white matter structure throughout adulthood, *Neuroimage*, **51** (2010), 943–951.

25. T. T. Brown, J. M. Kuperman, Y. Chung, et al., Neuroanatomical assessment of biological maturity, *Current Biol.*, **22** (2012), 1693–1698.

26. G. Erus, H. Battapady, T. D. Satterthwait, et al., Imaging patterns of brain development and their relationship to cognition, *Cerebral Cortex*, **25** (2014), 1676–1684.

27. A. Krizhevsky, I. Sutskever and G. E. Hinton, Imagenet classification with deep convolutional neural networks, in *Adv. Neural Inf. Process Syst.*, 2012, 1097–1105.

28. S. Ioffe and C. Szegedy, Batch normalization: Accelerating deep network training by reducing internal covariate shift, *arXiv preprint arXiv:1502.03167*.

29. J. Xing, K. Li, W. Hu, et al., Diagnosing deep learning models for high accuracy age estimation from a single image, *Patt. Recogn.*, **66** (2017), 106–116.

30. J. Guo, H. Du, J. Zhu, et al., Relative location prediction in ct scan images using convolutional neural networks, *Comput. Meth. Prog. Bio.*, **160** (2018), 43–49.

31. X. Glorot, A. Bordes and Y. Bengio, Deep sparse rectifier neural networks, in *Proceedings of the fourteenth international conference on artificial intelligence and statistics*, 2011, 315–323.

32. D. B. Larson, M. C. Chen, M. P. Lungren, et al., Performance of a deep-learning neural network model in assessing skeletal maturity on pediatric hand radiographs, *Radiology*, **287** (2017), 313–322.

33. J. L. Whitwell, Progression of atrophy in alzheimers disease and related disorders, *Neurotox Res.*, **18** (2010), 339–346.

34. F. Agosta, M. Pievani, S. Sala, et al., White matter damage in alzheimer disease and its relationship to gray matter atrophy, *Radiology*, **258** (2011), 853–863.

35. G. F. Busatto, G. E. Garrido, O. P. Almeida, et al., A voxel-based morphometry study of temporal lobe gray matter reductions in alzheimers disease, *Neurobiol. Aging*, **24** (2003), 221–231.

36. Z. Yao, Y. Zhang, L. Lin, et al., Abnormal cortical networks in mild cognitive impairment and alzheimer's disease, *Plos Comput. Biol.*, **6** (2010), e1001006.

AIMS Press